Gating currents from a Kv3 subfamily potassium channel: charge movement and modification by BDS-II toxin

Zhuren Wang[1], Brian Robertson[2] and David Fedida[1]

[1] *Department of Anaesthesiology, Pharmacology and Therapeutics, University of British Columbia, 2350 Health Sciences Mall, Vancouver, BC, Canada V6T 1Z3*

[2] *Neuroscience Research Group, Institute of Membrane and Systems Biology, Faculty of Biological Sciences, University of Leeds, Leeds LS2 9JT, UK*

Kv3 channels have a major role in determining neuronal excitability, and are characterized by ultra-rapid kinetics of gating and a high activation threshold. However, the gating currents, which occur as a result of positional changes of the charged elements in the channel structure during activation, are not well understood. Here we report a study of gating currents from wild-type Kv3.2b channels, expressed in human embryonic kidney (HEK) cells to facilitate high time-resolution recording. On-gating currents ($I_{g,on}$) had extremely rapid kinetics such that at +80 mV, the time constant for the decay of $I_{g,on}$ was only ∼0.3 ms. Decay of $I_{g,on}$ appeared mono-exponential at all potentials studied, and in support of this, the charge–voltage (Q–V) relationship was fitted with a single Boltzmann function, supporting the idea that only one charge system is required to account for the time course of $I_{g,on}$ and the voltage dependence of Q_{on}. The voltage ($V_{1/2}$) for half movement of gating charge was -8.4 ± 4.0 mV ($n = 6$), which closely matches the voltage dependence of activation of Kv3.2b ionic currents reported before. Depolarizations to more positive potentials than 0 mV decreased the amplitude and slowed the decay of the off-gating currents ($I_{g,off}$), suggesting that a rate-limiting step in opening was present in Kv3 channels as in *Shaker* and other Kv channels. Return of charge was negatively shifted along the potential axis with a $V_{1/2}$ of Q_{off} of -80.9 ± 0.8 mV ($n = 3$), which allowed ∼90% charge return upon repolarization to −100 mV. BDS-II toxin apparently reduced $I_{g,on}$, and greatly slowed the kinetics of $I_{g,on}$, while shifting the Q–V relationship in the depolarizing direction. However, the Q–V relationship remained well fitted by a single Boltzmann function. These data provide the first description of Kv3 gating currents and give further insight into the interaction of BDS toxins and Kv3 channels.

(Resubmitted 5 July 2007; accepted after revision 11 September 2007; first published online 13 September 2007)
Corresponding author D. Fedida: Department of Anaesthesiology, Pharmacology and Therapeutics, University of British Columbia, 2350 Health Sciences Mall, Vancouver, BC, Canada V6T 1Z3. Email: fedida@interchange.ubc.ca

Many neuronal types throughout the mammalian CNS, such as interneurones, are able to fire action potentials at high frequencies or follow high frequency inputs. Kv3 potassium channels have been identified as crucial components of the neuronal circuits capable of producing such responses, with their high activation threshold and remarkably fast activation and deactivation properties (Rudy *et al.* 1999; Rudy & McBain, 2001). These biophysical gating properties mirror those of certain endogenous neuronal K^+ currents (Brew & Forsythe, 1995; Perney & Kaczmarek, 1997; Southan & Robertson, 2000; Lien & Jonas, 2003) and thereby suggest that Kv3 channels can confer a 'fast spiking' phenotype to many CNS neurons (Wang *et al.* 1998; Martina *et al.* 1998; Southan & Robertson, 2000; Lien & Jonas, 2003). Some previous gating current recordings suggest that fundamental differences in the kinetics of voltage-dependent charge movement might underlie the rapid kinetics of Kv3 ionic currents. Comparison between Kv2.1 and Kv3.1 gating currents recorded using macropatch methods in *Xenopus* oocytes demonstrated a remarkable acceleration of the kinetics of charge movement during activation and deactivation in Kv3.1 channels, such that the onset of on-gating currents ($I_{g,on}$) could not be well resolved by patch clamp recording (Shieh *et al.* 1997).

In addition, a reduction in the amplitude and slowing in the kinetics of off-gating currents ($I_{g,off}$) after larger depolarizations, that is a general phenomenon reported in *Shaker* and Kv channel gating current studies (Perozo *et al.* 1992, 1993; Chen *et al.* 1997; Yang *et al.* 1997; Wang *et al.* 1999; Wang & Fedida, 2001), was not present in the Kv3.1 gating current recordings (Shieh *et al.* 1997). Rapid kinetics of gating charge movement were also apparent in previous gating current recordings from HEK cells expressing a high

 DOI: 10.1113/jphysiol.2007.140145

density of Kv3.2b P468W mutant channels, as was a lack of gating charge slowing on repolarization (Yeung *et al.* 2005). Although Kv3 channels apparently show these differences in the gating kinetics from *Shaker* and Kv1 channels, the molecular mechanisms have not been fully explored, partly due to the difficulty in making such measurements.

BDS (blood-depressing substance) toxins are sea anemone peptides from *Anemonia sulcata* (Diochot *et al.* 1998) which inhibit Kv3 channels with high affinity when applied to the extracellular face of the membrane (Diochot *et al.* 1998; Yeung *et al.* 2005). BDS toxins bound to the S3b and S4 segments hinder voltage sensor movement (Yeung *et al.* 2005), and shift the voltage dependence of activation of Kv3 channels to more depolarizing potentials, analogous to the interaction of hanatoxin and Kv2.1 channels (Swartz & MacKinnon, 1997*a*,*b*; Lee *et al.* 2003). Unlike pore-blocking toxins that directly interfere with ion conduction (Miller, 1995), BDS toxins may inhibit Kv3 channels by modifying the energetics of activation (Swartz & MacKinnon, 1995; Lee *et al.* 2003). This mechanism is supported by our prior gating current study of Kv3.2b P468W mutant channels where we demonstrated that the charge–voltage relationship is shifted +25 mV by 1 μM BDS-II toxin, which matches the shift of the voltage dependence of activation (Yeung *et al.* 2005).

Here we have characterized the gating currents of Kv3.2b wild-type channels at high time resolution in order to compare these data with the accelerated kinetics of gating current and the lack of gating charge slowing observed in Kv3.1 channels expressed in *Xenopus* oocytes (Shieh *et al.* 1997), and in Kv3.2b P468W channels expressed in HEK cells (Yeung *et al.* 2005). The successful recording of gating currents has allowed the measurement of the voltage dependence and the kinetics of gating charge movement during activation and deactivation, and provided the first systematic description of Kv3 gating currents. Moreover, changes in the kinetics of gating charge movement as well as the voltage dependence of charge distribution after application of BDS-II offer insight into interaction of the channel proteins and the toxin.

Methods

Molecular biology and cell culture

The mammalian expression vector pcDNA3 was used for expression of rat Kv3.2b channels (Luneau *et al.* 1991) and was sequenced to check for errors before being used in transient transfections of HEK 293 cells. The cells were grown in minimal essential medium (MEM) with 10% fetal bovine serum, at 37°C in an air–5% COB_2 incubator. For transient transfection, HEK cells were plated at 20–30% confluence on sterile glass coverslips in 25 mm Petri dishes overnight. Kv3.2b channel DNA was incubated with enhanced green fluorescent protein (eGFP) in order to identify the transfected cells efficiently (2 μg of eGFP, 2 μg of channel DNA) and 3 μl of Lipofectamine 2000 (Invitrogen) in 100 μl of serum-free media for 30 min, and then added to the dishes containing HEK 293 cells in 2 ml of MEM with 10% fetal bovine serum. After 5 h incubation, the culture medium was changed and then cells were incubated overnight before recording. Cells that expressed GFP were selected for patch clamp experiments.

Electrophysiology

Coverslips containing adherent cells were removed from the incubator before experiments and placed in a superfusion chamber (volume 250 μl) containing the control bath solution at ambient temperature (22–23°C). The bath solution was exchanged by switching the perfusates at the inlet of the chamber, with complete bath solution changes taking 5–10 s. Whole-cell current recording and data analysis were done using an Axopatch 200B amplifier and pCLAMP 8 software (Axon Instruments, Union City, CA, USA). Patch electrodes were fabricated using thin-walled borosilicate glass (World Precision Instruments, FL, USA), routinely coated with Sylgard (Dow Corning) and fire polished to reduce electrode capacitance and improve seal resistance. Electrodes had resistances of 1–3 MΩ when filled with the filling solutions. Capacity compensation was routinely used in all whole-cell recordings. Measured series resistance was between 1 and 3 MΩ for all recordings. When the series resistance changed during the course of an experiment, data were discarded. In gating current recording a '*P*/−6' protocol was routinely used for the online subtraction of the leakage and capacitive currents. The potential used for delivery of leak subtraction pulses was −90 to −110 mV. Data were filtered using a 4-pole Bessel filter with a cut-off frequency (f_c) of 10 kHz, and sampled at 100 kHz. For some experiments, as indicated in the text and figure legends, the gating current was recorded using 60% series resistance compensation, a 100 kHz filter and a 330 kHz sampling rate. Membrane potentials have not been corrected for small junction potentials that arose between bath and pipette solutions.

All charge measurements (Q_{on} and Q_{off}) were obtained by integrating the on- ($I_{g,on}$) and off-gating ($I_{g,off}$) current over sufficient time to allow gating currents to return to the baseline. The charge–voltage (Q–V) relationships were determined from Q_{on} or Q_{off} elicited during or after 12 ms pulses to a variable test potential. The Q_{on} or Q_{off} for each test potential was normalized to the maximum Q_{on} or Q_{off}, respectively. The voltage dependence of gating charge movement was determined by fitting a single Boltzmann function to the normalized gating charge (Q) values. The equation used to fit the data was: $Q = Q_{max}/\{1 + \exp[-(V - V_{½})/k]\}$, where Q_{max} is the maximum gating charge, V the membrane potential, $V_{½}$ the voltage for half charge movement, and k the slope factor.

The time course of the decaying phase of on- and off-gating currents was fitted with a single exponential function: $a + b\exp(-x/t)$, where a represents an offset, b is the current amplitude and t is the time constant. During the present study we report time constants of off-gating current decay (τ_{off}) of ~0.8 ms, much slower than the mean capacity transient decay rates $58 \pm 0.3\ \mu$s, so that recording bandwidth does not appear to be a limiting factor in the measurements. Throughout the text data are presented as mean ± S.E.M.

For recordings of gating currents, patch pipettes contained (mM): *N*-methyl D-glucamine (NMG^+), 140; $MgCl_2$, 1; EGTA, 10; Hepes, 10; and was adjusted to pH 7.2 with HCl. The bath solution contained (mM): tetraethylammonium (TEA^+), 140; Hepes, 10; dextrose, 10; $MgCl_2$, 1; $CaCl_2$, 1; and was adjusted to pH 7.4 with HCl. All chemicals were from Sigma Aldrich Chemical Co. BDS-II toxin, isolated from *Anemonia sulcata*, was purchased from Alomone Laboratories (Jerusalem, Israel). BDS-II was applied externally via bath superfusion.

Results

Gating currents from HEK cells expressing Kv3.2b channels

Rat Kv3.2b channels (Luneau *et al.* 1991) were transiently expressed in HEK cells and the non-permeant cations, NMG^+ and TEA^+, were used in the intracellular and extracellular solution, respectively, to replace permeant K^+ and Na^+ ions. Given that Kv3 channels are characterized by ultra-rapid kinetics of gating (Rudy *et al.* 1999; Rudy & McBain, 2001), the initial experiments examined the properties of the recording system. A typical uncorrected capacity transient recorded from an untransfected HEK cell during a 150 mV step pulse decayed with a time constant of 54 μs ($58 \pm 3\ \mu$s, $n = 5$; Fig. 1*A*), similar to values reported before (Hesketh & Fedida, 1999). Data recorded from a HEK cell expressing Kv3.2b channels are shown in Fig. 1*B*. The cell was clamped at −100 mV and depolarized to +80 mV, the leak current was subtracted using a standard ($P/-6$) protocol, and the data were sampled at 100 kHz through a 10 kHz f_c filter (Wang *et al.* 1999; Wang & Fedida, 2001, 2002). The continuous black line is the $I_{g,on}$ during the depolarization, and has a time to peak (t_{peak}) of 240 μs. The grey line shows the current after application of 60% series resistance compensation, and final filtering at 20 kHz. This reduced t_{peak} to < 170 μs, but did not significantly affect the amount of charge moved during the depolarization or the time course of $I_{g,on}$ decay to the baseline, as seen from the two current recordings (Fig. 1*B*, $n = 4$).

Current records in Fig. 1*C* and *D* show Kv3.2b gating currents before and after $P/-6$ online leak subtraction, respectively. It can be seen that the small-maintained current component present during the depolarization and repolarization in Fig. 1*C* was reduced. The transient current components were otherwise little changed by the leak subtraction protocol.

The kinetics of gating currents recorded from Kv3.2b channels

On-gating currents appeared as transient outward current deflections during depolarizations positive to −40 mV which increased in amplitude with larger depolarizations, and decayed more quickly (Fig. 2*A*). The $I_{g,on}$ exhibited a rising phase that was barely visible for small depolarizations but became pronounced at larger depolarizations, similar to that seen in *Shaker* and other Kv channels (Bezanilla *et al.* 1991, 1994; Perozo *et al.* 1992; Chen *et al.* 1997). Clearly, the on-gating currents decayed very rapidly during depolarizing pulses. At +80 mV the $I_{g,on}$ decayed to the zero current level in only ~1.2 ms, a much briefer transient current than that reported in *Shaker* and other Kv channels, such as Kv1.5 (Wang *et al.* 1999; Claydon *et al.* 2007). When pulsed back to −100 mV, the off-gating current ($I_{g,off}$) represents the return of gating elements as channels deactivate. In Fig. 2*A*, the $I_{g,off}$ are seen as downward current deflections after depolarizing pulses. In contrast to $I_{g,on}$, the $I_{g,off}$ time course was similar to that described in *Shaker* and Kv channels. After small depolarizations (at potentials < 0 mV), the charge return was fast and the $I_{g,off}$ increased in amplitude with the enhancement of depolarization. For intermediate depolarizations, $I_{g,off}$ had a fast component followed by a smaller slower component. At depolarizations > +20 mV, the peak of $I_{g,off}$ became smaller, with a rising phase and a very slow decay. However, the rising phase of $I_{g,off}$ after the larger depolarizations was not as prominent as in *Shaker* (Bezanilla *et al.* 1994) or Kv1.5 channels (Wang *et al.* 1999).

The time- and voltage-dependent movement of gating charge (Q_{on}) as channels progress towards the open state, and the subsequent relaxation of charge upon channel closing (Q_{off}) are shown in Fig. 2*B*. As expected, Q_{on} increased in amplitude and moved faster at +80 than 0 mV, but for Q_{off}, although the amplitude was larger at +80 mV, less change was found in the already slowed kinetics. The averaged ratio of Q_{off} over Q_{on} was close to 1.0 over the range of potentials from −40 mV to −10 mV and ~0.9 when the potential was 0 mV and above (Fig. 2*C*). The relaxation of $I_{g,off}$ (τ_{off}) was mono-exponential between −40 and −20 mV and from +20 to +80 mV. Over the range of intermediate depolarizations (from −10 to +10 mV), the relaxation of $I_{g,off}$ was fitted with a bi-exponential function (Fig. 2*D*). The relaxation of off-gating current became significantly

slower with increasing depolarization, as τ_{off} increased from ~0.7 ms to ~5 ms over the range of potentials studied (Fig. 2*D*). These results are similar to those from wild-type and pore mutants of *Shaker* and Kv channels (Perozo *et al.* 1992, 1993; Chen *et al.* 1997; Yang *et al.* 1997), where Q_{off} is smaller and the charge return becomes dramatically slowed when the depolarization crosses the threshold of activation, but clearly different from the previously reported gating currents of Kv3.1 expressed in oocytes (Shieh *et al.* 1997) and Kv3.2b P468W mutant channels expressed in HEK cells (Yeung *et al.* 2005) that lack this slowing.

Voltage dependence of the gating charge movement in Kv3.2b channels

The voltage dependence of gating charge movement during activation and deactivation in Kv3.2b channels was analysed as shown in Fig. 3. The cell was held at −150 mV and depolarized to potentials between −60 and +80 mV for 12 ms to record $I_{g,on}$. Then the membrane potential was stepped back to −150 mV and the $I_{g,off}$ was also recorded (Fig. 3*A*). The Q_{on} was normalized to the maximum value and plotted as a function of potential in Fig. 3*C* (filled circles). It is apparent that the charge distribution is symmetrical in Kv3.2b channels, and that

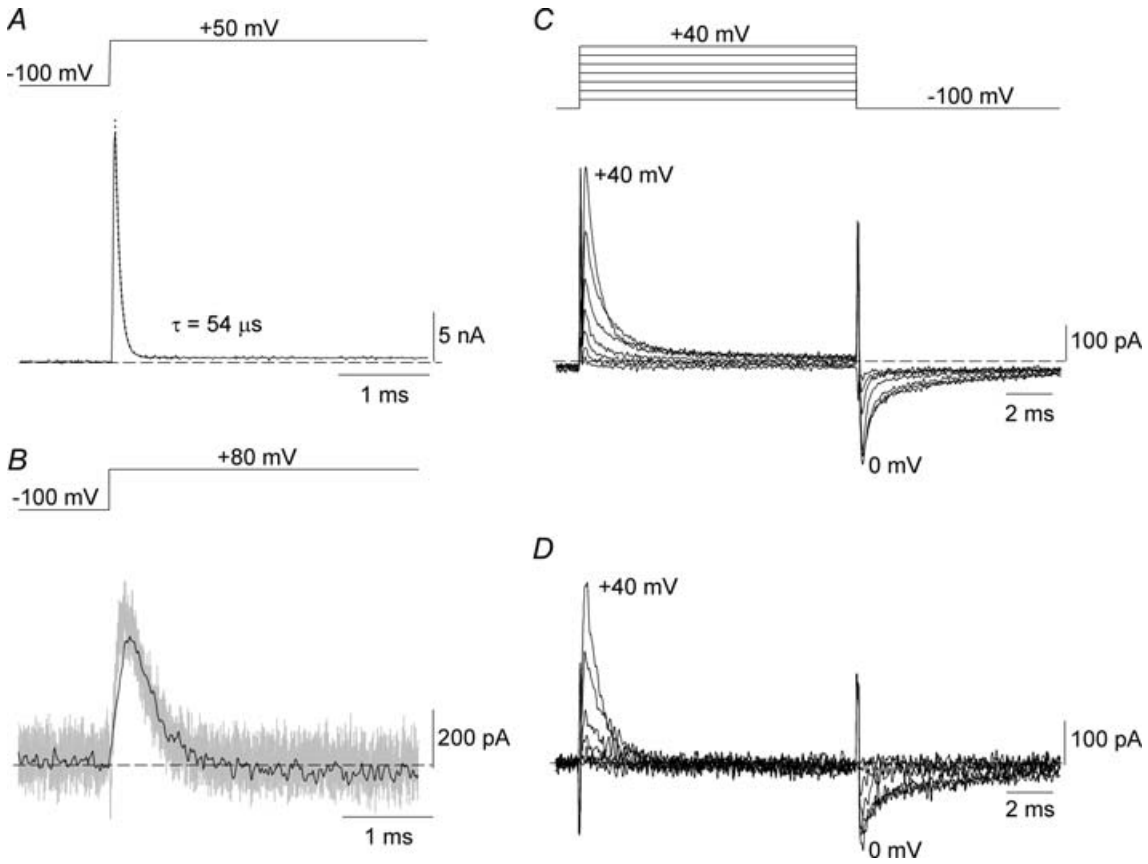

Figure 1. Recording gating currents from HEK cells expressing Kv3.2b channels
A, an uncorrected capacity transient from an untransfected HEK cell during a voltage step from −100 mV to +50 mV as shown at the top. A monoexponential decay function is superimposed as a dotted line ($\tau = 54$ μs). *B*, on-gating current tracings ($I_{g,on}$) from Kv3.2b channels elicited by the voltage pulse protocol above. The cell was held at −100 mV and depolarized to +80 mV, and currents were recorded with both capacity compensation and leak current subtraction as described in Methods. Grey: a current trace recorded using 60% series resistance compensation, with a 100 kHz f_c filter at a 330 kHz sampling frequency. For presentation, the data were further filtered at 20 kHz offline. Black: without series resistance compensation, filtered at 10 kHz, and sampled at 100 kHz. Both current tracings were obtained from the same cell. *C* and *D*, gating currents recorded from the same cell before (*C*), and after (*D*) the application of leak-current subtraction. The pulse protocol used to elicit gating currents is shown at the top of *C*. The cell was held at −100 mV and depolarized at 0.5 Hz to potentials between −80 and +40 mV in 20 mV steps. The short dashed lines denote the zero current level in this and subsequent figures.

the Q_{on}–V relationship can be fitted with a single Boltzmann function. The voltages for half movement of the gating charge ($V_{½}$) and the slope factor (k) were -8.4 ± 4.0 mV and 12.2 ± 1.6 mV ($n = 6$), respectively. At -150 mV, the return of gating charge was rapid and complete in 10 ms (Fig. 3*A*), and when the normalized Q_{off} values were fitted with a Boltzmann function, the parameters were almost identical to the Q_{on}–V curve data (Fig. 3*C*, filled triangles). The $V_{½}$ and slope factor (k) were -6.0 ± 3.5 mV and 13.8 ± 1.3 mV ($n = 6$), respectively. This symmetrical distribution of the gating charge is unlike that found in *Shaker* and Kv1.5 channels, where the charge distribution is asymmetrical, and usually fitted to a double-Boltzmann function that indicates the existence of two activating charge systems (Bezanilla *et al.* 1994; Hesketh & Fedida, 1999). In addition, these data indicate that the voltage dependence of the gating charge movement during depolarization can be analysed equivalently by the measurement of Q_{on} during depolarization or Q_{off} at very negative repolarizing potentials.

The voltage dependence of charge movement during repolarization was measured using the protocol illustrated in Fig. 3*B*. After a depolarization to +80 mV for 12 ms, to fully move the gating charge associated with channel activation (cf. Fig. 3*C*), the membrane was repolarized to various potentials between -150 and -40 mV for long enough to allow the current decay to reach an apparent

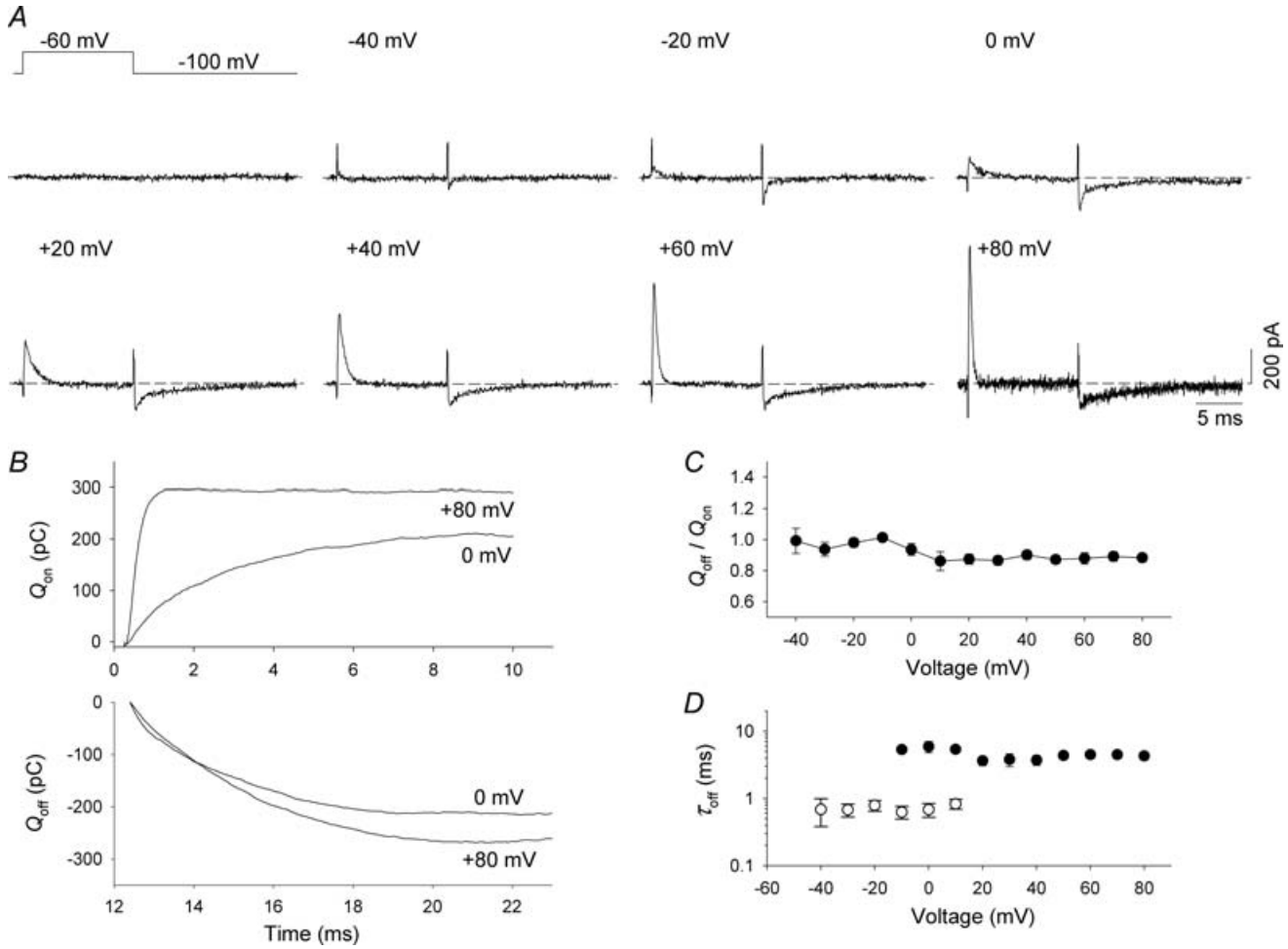

Figure 2. Measurement of the gating currents from Kv3.2b channels
A, current tracings recorded from a HEK cell expressing Kv3.2b channels. The cell was held at -100 mV and pulsed to the potentials as indicated above the current trace. *B*, time course of the gating charge movement in Kv3.2b channels during depolarization (top) to potentials indicated and repolarization (bottom). The amount of charge displaced during depolarization and repolarization (Q_{on} and Q_{off}) was obtained from the time integral of the $I_{g,on}$ and $I_{g,off}$ shown in *A*. *C*, averaged ratio of Q_{off}/Q_{on} as a function of the pulse potentials, from data as in *A* ($n = 8$). *D*, time constants (τ_{off}) for the relaxation of $I_{g,off}$ plotted against the pulse potentials, from data as in *A* ($n = 8$). A mono-exponential function was used to fit the relaxation of $I_{g,off}$ except for depolarizations between -10 mV and +10 mV, where the relaxation phase of $I_{g,off}$ was best fitted with a bi-exponential function.

baseline. The Q_{off} was obtained by integrating the $I_{g,off}$ at these different potentials and, after normalization, was plotted in Fig. 3*C* (bottom panel, filled squares) and fitted with a Boltzmann function. The Q_{off}–V curve was shifted to hyperpolarizing potentials compared with the charge relationships plotted in the upper panel, and this was caused by a failure of complete charge return at potentials positive to −100 mV during the repolarizing pulse, due to the voltage-dependent kinetics of $I_{g,off}$. The time constant of decay (τ_{off}) increased from ∼0.8 ms at −190 mV to ∼5 ms at −70 mV (Fig. 3*D*). This can be clearly seen in the current records in Fig. 3*B*, where, at the end of the protocol, a return to the holding potential of −150 mV elicited small transient off-gating currents as the remaining charge was allowed to return to rest.

Kinetics of the gating charge movement upon depolarization in Kv3.2b channels

On-gating currents measured from *Shaker* channels decay in a double exponential manner at intermediate depolarizations (Bezanilla *et al.* 1994). In Kv1.5 channels, $I_{g,on}$ also shows complex kinetics, having more rounded peaks and plateaus at the intermediate depolarizations (Hesketh & Fedida, 1999). Separation of the gating

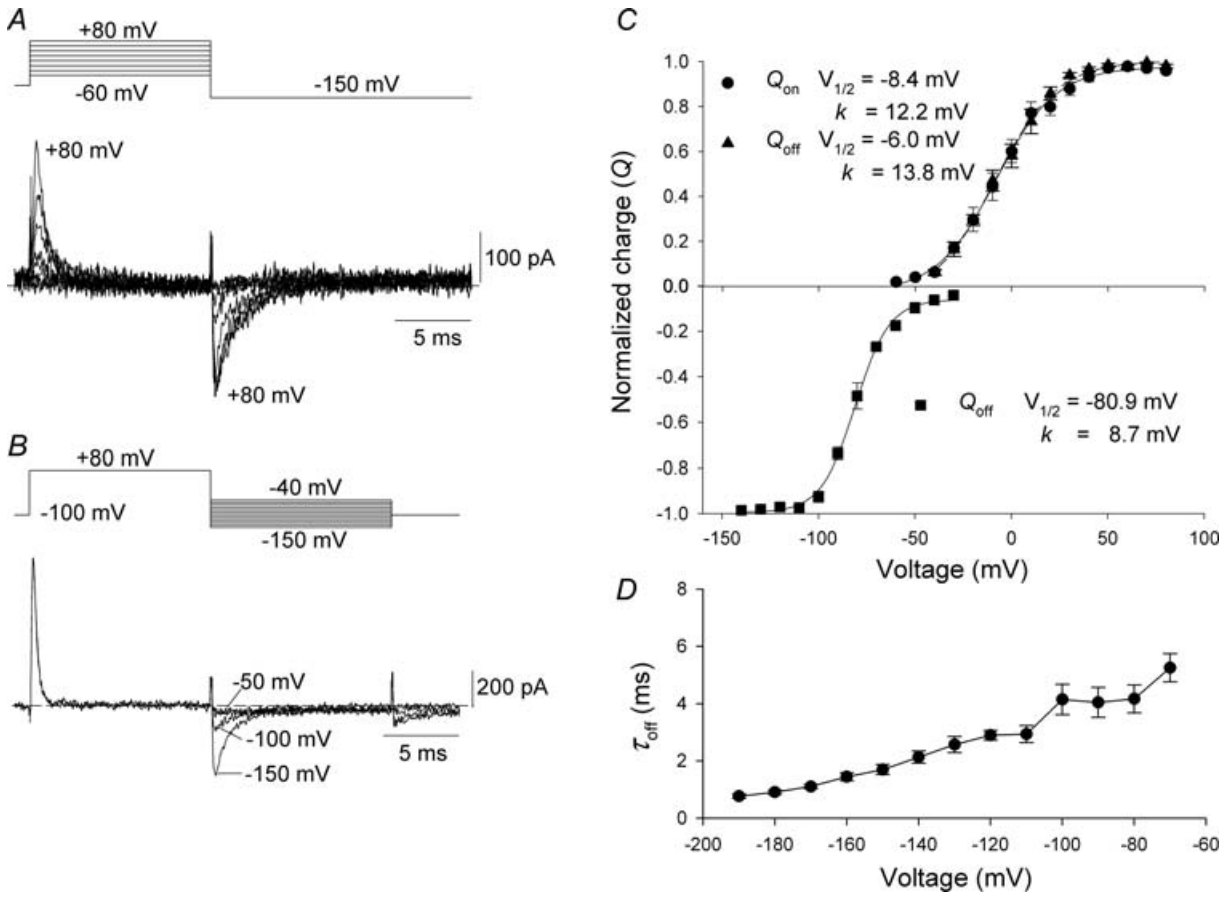

Figure 3. Voltage dependence of gating charge movement in Kv3.2b channels
A, gating currents recorded during 12 ms depolarizations from −150 mV to potentials between −60 mV and +80 mV in 20 mV steps applied at 0.5 Hz. *B*, gating currents recorded after depolarizations to +80 mV upon repolarization to potentials between −40 mV and −150 mV in 10 mV steps (protocol at top), pulses applied at 0.5 Hz. *C*, top, voltage dependence of gating charge movement during depolarization. The Q_{on} and Q_{off} from the experiments shown in *A* were normalized to the values obtained with a +80 mV depolarization. The normalized Q_{on} (●) and Q_{off} (▲) was plotted against the pulse potential and fitted with a single Boltzmann function ($n = 6$). The $V_{1/2}$ was −8.4 ± 4.0 mV and −6.0 ± 3.5 mV and slope factor (k) was 12.2 ± 1.6 mV and 13.8 ± 1.3 mV, for Q_{on} and Q_{off}, respectively. Bottom, voltage dependence of the charge movement during repolarization. The Q_{off} from the experiments as shown in *B* was normalized to the value obtained at −150 mV. The normalized Q_{off} (■) was plotted against the membrane potential and fitted with a single Boltzmann function ($n = 3$) with a $V_{1/2}$ of −80.9 ± 0.8 mV and a slope factor (k) of 8.7 ± 0.4 mV. *D*, time constants (τ_{off}) for the relaxation of $I_{g,off}$ plotted as a function of repolarizing potential, from data as in *B* ($n = 6$). The relaxation phase of $I_{g,off}$ was fitted with a mono-exponential function.

currents into two charge systems fitted with a double Boltzmann distribution, and subsequent modelling allowed the waveforms to be well described in both systems. When Kv3.2b gating currents were inspected (Fig. 2*A*), however, it was apparent that there was only a single decay phase to $I_{g,on}$ regardless of the amplitude of depolarization. The current data in Fig. 4*A* show mono-exponential fits to the decaying phase of Kv3.2b $I_{g,on}$ at small (−10 mV), intermediate (0 and +20 mV) and large depolarizations (+60 mV). The time constants are plotted against voltage in Fig. 4*B*, and between −30 mV and +20 mV the currents tend to decay more slowly with time constants between 1 and 2 ms, whereas for larger depolarizations (> +20 mV) the current decay becomes much faster. So that, in addition to the monophasic nature of the decay of $I_{g,on}$, the data also show that Kv3.2b gating charge moves quite rapidly, especially during larger depolarizations (Shieh *et al.* 1997; Yeung *et al.* 2005). For example, at +80 mV, the time constant for the decaying phase of $I_{g,on}$ is ∼0.3 ms (Fig. 4*B*). The slowest charge movement occurs around 0 mV with a time constant of ∼2 ms.

The charge distribution was also estimated from these data by multiplying the fitted amplitude by the time constants (Bezanilla *et al.* 1994) to obtain the relationship plotted in Fig. 4*C*. The experimental points can be well fitted to a single Boltzmann function, with a $V_{½}$ and k of −8.2 ± 1.2 mV and 6.7 ± 0.7 mV ($n = 4$), respectively. The values are close to those obtained by integration of the entire transients (Fig. 3*C*) which supports the validity of the exponential analysis in Fig. 4*A*, and the idea of a single activating charge system in Kv3.2b gating.

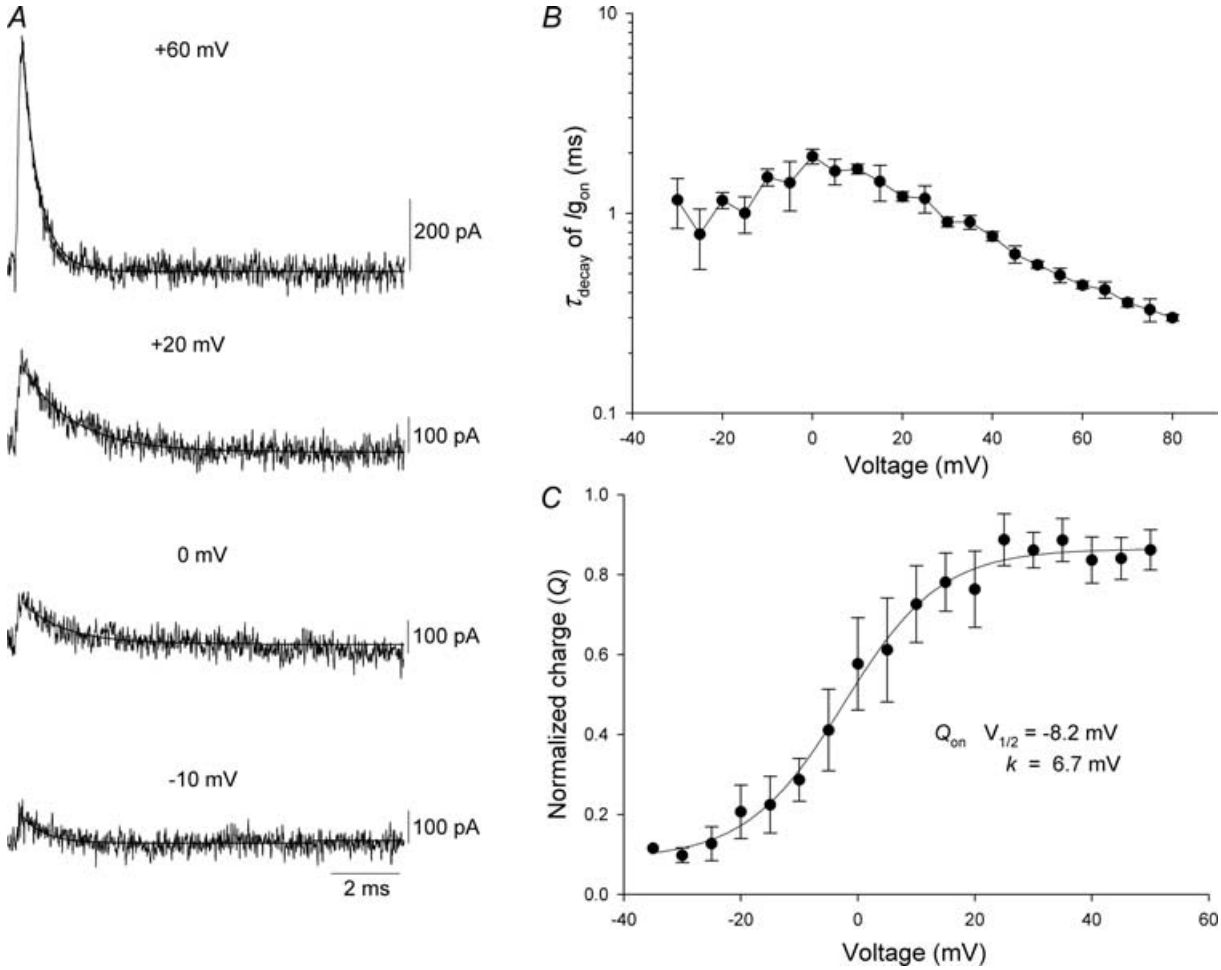

Figure 4. Kinetic properties of $I_{g,on}$ in Kv3.2b channels
A, $I_{g,on}$ at −10, 0, +20 and +60 mV from a holding potential of −100 mV. Capacity compensation, leak subtraction and 60% series resistance compensation were applied, and current was sampled at 330 kHz after filtering at 100 kHz. For presentation, the data were further filtered at 20 kHz offline. Superimposed continuous lines are mono-exponential fits to the decaying phase of $I_{g,on}$. *B*, averaged time constants (τ_{decay}) for the decay of $I_{g,on}$ as a function of pulse potential ($n = 9$). *C*, the *Q*–*V* curve obtained by fitting the integral of the exponential decay of $I_{g,on}$ to a single Boltzmann function. The $V_{½} = -8.2 \pm 1.2$ mV, and the slope factor (k) = 6.7 ± 0.7 mV ($n = 4$).

Modulation of Kv3.2b gating currents by BDS-II toxin

As BDS toxins bind to the S3b and S4 segments in the Kv3 channel α-subunit (Yeung *et al.* 2005), the movement of 'voltage sensor' domains during activation and deactivation should be directly affected, and potentially could give further insight into the mechanisms of Kv3.2b gating. Gating currents recorded from Kv3.2b in the presence of 1 μM BDS-II in the bathing solution are shown in Fig. 5*A*. Compared with control data in Fig. 2*A*, several changes in the on-gating currents are clear. First, the $I_{g,on}$ does not appear until the membrane is depolarized to -20 mV. Second, a slowly decaying component of $I_{g,on}$ can be seen after the initial spike during larger depolarizations. Third, the $I_{g,off}$ becomes clearly larger than the $I_{g,on}$ during the prepulse. The appearance of the slowly decaying component in $I_{g,on}$ induced by BDS-II toxin was studied by fitting the relaxation time course of depolarizations below +50 mV to a mono-exponential, and depolarizations at +50 mV and above, where the slow decaying component becomes apparent, to a double exponential function (Fig. 5*B*). Both fast and slow time constants are voltage sensitive (Fig. 5*C*), with fast time constants similar to those in control (Fig. 4*B*), and

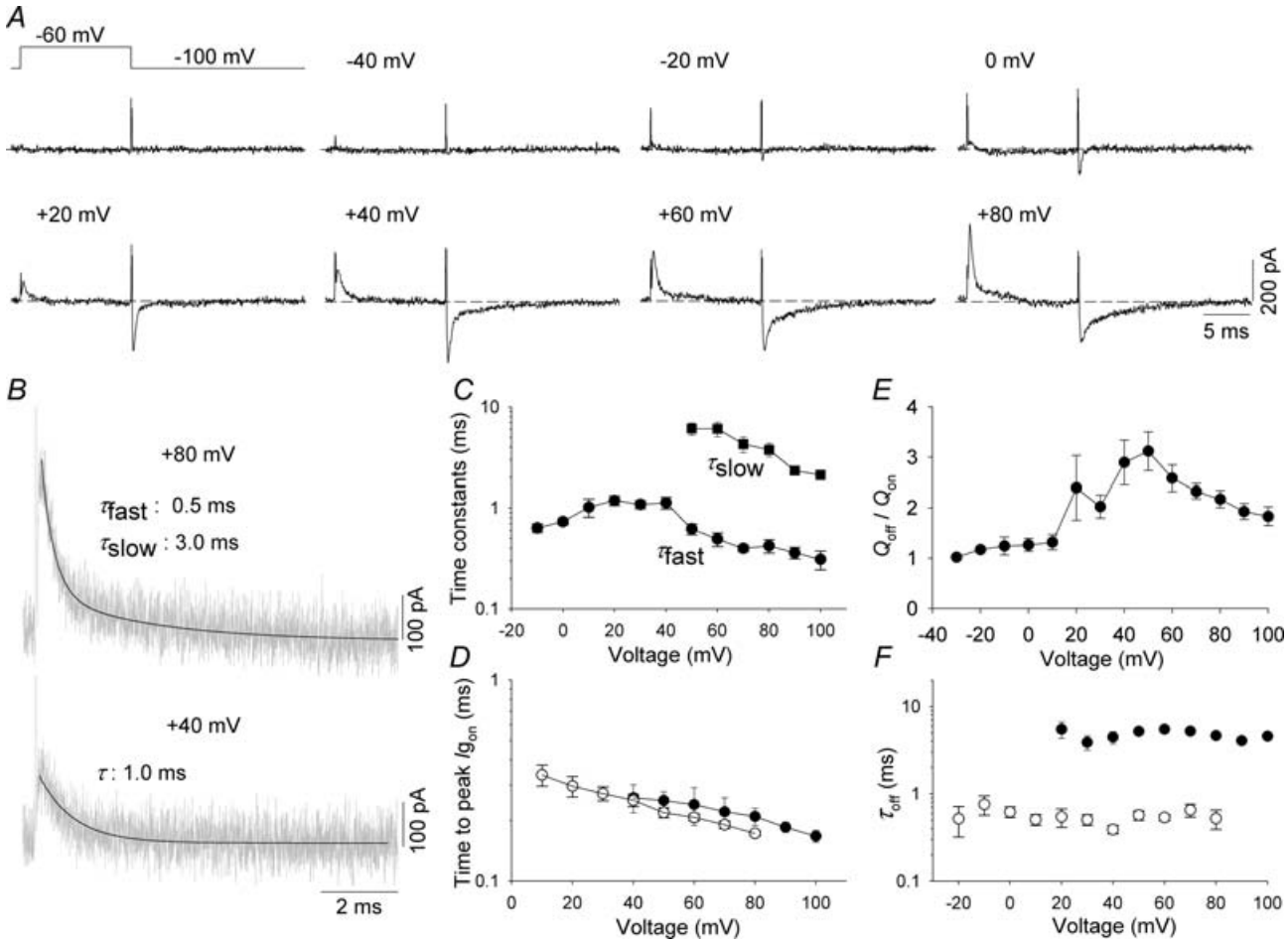

Figure 5. Kv3.2b gating currents in the presence of BDS-II
A, current tracings from Kv3.2b channels with 1 μM BDS-II toxin in the bath. The cell was held at -100 mV and pulsed to the potentials as indicated above the current traces. *B*, $I_{g,on}$ at +40 and +80 mV from a holding potential of -100 mV. Capacity compensation, leak subtraction and 60% series resistance compensation were applied and currents were filtered at 100 kHz and sampled at 330 kHz. For presentation, the data were further filtered at 20 kHz offline. Superimposed continuous lines are mono-exponential (+40 mV) or bi-exponential (+80 mV) fits to the decay of $I_{g,on}$ with fast and slow time constants (τ_{fast} and τ_{slow}). *C*, averaged τ_{fast} and τ_{slow} of the decaying phase of $I_{g,on}$ as a function of pulse potential ($n = 5$–8). *D*, averaged time to peak $I_{g,on}$ from the beginning of the pulse in the presence (●) and absence (○) of 1 μM BDS-II plotted as a function of potential, from data as in *A* ($n = 4$). *E*, the averaged ratio of Q_{off}/Q_{on} as a function of pulse potential, from data as in *A* ($n = 5$). *F*, the time constants (τ_{off}) for the relaxation of $I_{g,off}$ plotted as a function of pulse potential, from data as in *A* ($n = 7$). A mono-exponential function was used to fit $I_{g,off}$ except between +20 mV and +80 mV, where a bi-exponential function was used.

the slow time constants almost 10-fold slower. It is notable that the slowly decaying component remains separated from the fast component, even at very large depolarizations (+100 mV).

The rising phase of $I_{g,on}$ remained very rapid in the presence of 1 μM BDS-II. The time to peak $I_{g,on}$, i.e. the time from the beginning of the pulse to the peak of $I_{g,on}$, was measured in the absence and presence of 1 μM BDS-II and plotted against potential (Fig. 5*D*). The voltage dependence of the time to peak $I_{g,on}$ was not altered significantly by BDS-II toxin.

The average ratio of Q_{off} to Q_{on} was significantly greater than 1.0 at potentials more positive than +10 mV (Fig. 5*E*). The largest ratio value (~3) was observed at +50 mV, and then the ratio decreased again with larger depolarizations. This voltage-dependent inhibition of $I_{g,on}$ is reminiscent of the inhibition of ionic current by BDS-II, which is more marked between +20 and +80 mV (Yeung *et al.* 2005). Few significant changes in $I_{g,off}$ were observed in the presence of the toxin, except for a more clearly bi-exponential relaxation of $I_{g,off}$ over a wider potential range than in control (Fig. 5*F*).

The voltage dependence of charge movement in the presence of 1 μM BDS-II toxin is shown in Fig. 6, in the same format as control data (Fig. 3). Because of the minor effect of BDS-II on deactivation and $I_{g,off}$ (see below), the measurement of Q_{off} becomes the only way to measure the charge moved by depolarizing pulses (Lee *et al.* 2003; Yeung *et al.* 2005). Normalized Q_{off} (Fig. 6*A*) values were plotted *versus* pulse potential and fitted with a single

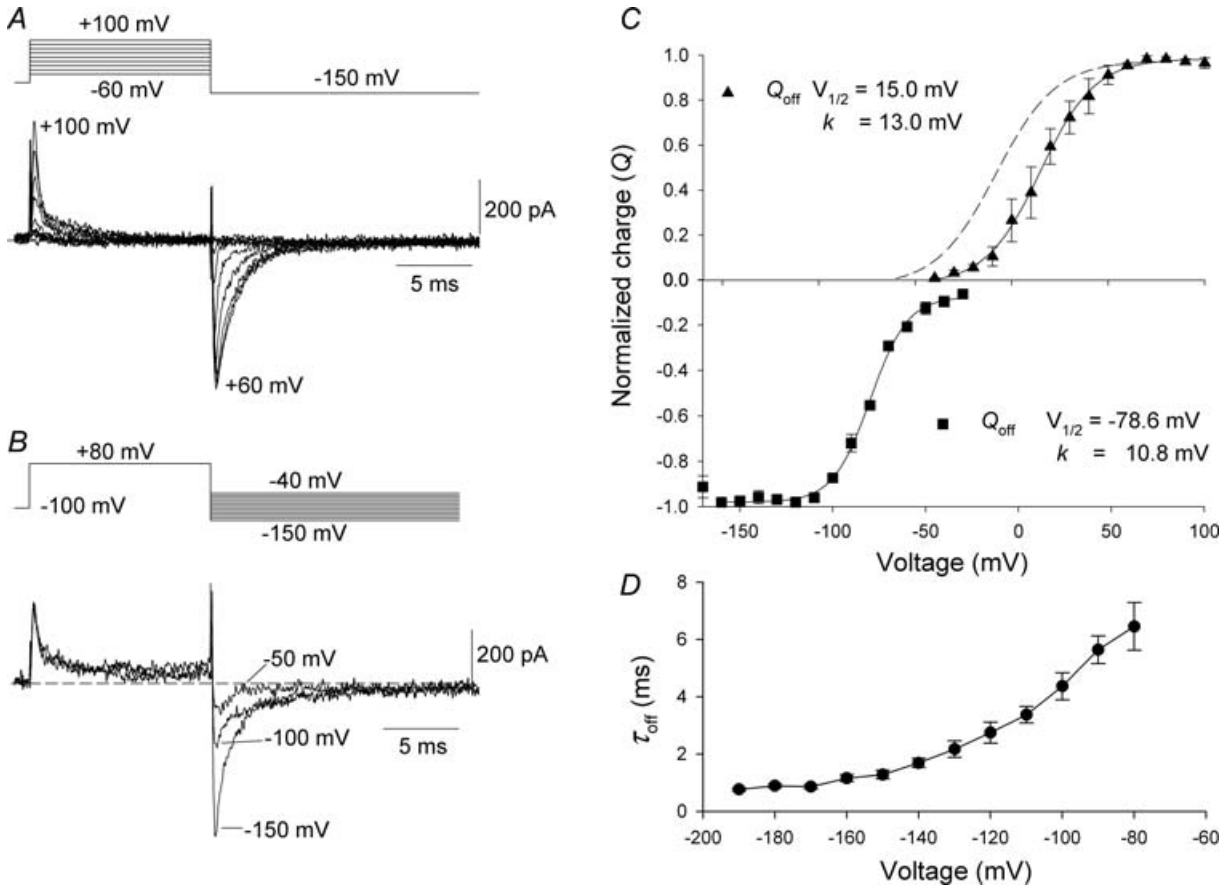

Figure 6. Voltage dependence of charge movement in the presence of 1 μM BDS-II
A, gating currents recorded during 12 ms depolarizations from −150 mV to between −60 mV and +100 mV in 20 mV steps (top) applied at 0.5 Hz. *B*, gating currents recorded during a depolarization to +80 mV for 12 ms followed by repolarization to between −40 mV and −150 mV in 10 mV steps. The pulses were applied at 0.5 Hz. *C*, top, voltage dependence of gating charge movement during depolarizations in the presence of 1 μM BDS-II toxin. Q_{off} from the experiments shown in *A* was normalized, plotted, and fitted with a single Boltzmann function, with a $V_{1/2}$ of 15.0 ± 5.8 mV and a slope factor (k) of 13.0 ± 0.6 mV ($n = 4$). The control Q_{on}–V curve from Fig. 3*C* is duplicated here as the dashed line. Bottom, voltage dependence of the charge movement during repolarization in the presence of 1 μM BDS-II toxin. The Q_{off} from the experiment shown in *B* was normalized to the value obtained at −150 mV and plotted against the pulse potential during repolarization. The $V_{1/2}$ was −78.6 ± 0.7 mV and the slope factor (k) was 10.8 ± 1.0 mV ($n = 5$). *D*, mono-exponential time constants (τ_{off}) for the relaxation of $I_{g,off}$ plotted as a function of repolarizing potential, from data as in *B* ($n = 6$).

Boltzmann function (Fig. 6*C*). The $V_{1/2}$ and slope factor (k) for the Q_{off}–V curve was 15.0 ± 5.8 mV and 13.0 ± 0.6 mV ($n = 4$), respectively, a 23 mV depolarizing shift from the control. The unchanged slope factor (k) implied that the equivalent gating charge sensed by the channels in the presence of BDS-II was unaltered from control (Fig. 3*C*). Neither the voltage dependence of charge return upon repolarization, nor the time constants for the relaxation of $I_{g,off}$ (τ_{off}) were significantly changed by BDS-II (Fig. 6*C* and *D*), further suggesting that the toxin has little effect on the deactivation process. The Q_{off}–V curve measured from experiments such as that shown in Fig. 6*B* had a $V_{1/2}$ of −78.6 ± 0.7 mV and a slope factor (k) of 10.8 ± 1.0 mV ($n = 5$) (Fig. 6*C*, bottom).

Discussion

Kv3.2b on-gating currents

On-gating current waveforms from rat Kv3.2b channels share several features in common with gating currents from *Shaker* (Perozo *et al.* 1992, 1993; Bezanilla *et al.* 1994; Yang *et al.* 1997) and other Kv channels, such as Kv1.5 (Fedida *et al.* 1996; Chen *et al.* 1997; Wang *et al.* 1999) and Kv2.1 channels (Taglialatela & Stefani, 1993; Shieh *et al.* 1997; Lee *et al.* 2003). Kv3.2b $I_{g,on}$ waveforms consistently have a rising phase followed by a decaying phase that becomes faster with depolarization (Figs 4*A* and 5*B*), highlighting a conserved voltage-dependent gating mechanism in which initial transitions are slower and/or carry less charge than subsequent gating transitions (Bezanilla & Stefani, 1994). In addition, the decay of $I_{g,on}$ is fast for small depolarizations, it slows for intermediate depolarizations, and for larger depolarizations (> 0 mV), the decay becomes fast again (Fig. 4). However, several differences between $I_{g,on}$ from Kv3.2b and those from other channels are also clear. The kinetics of the gating current transients appear much faster than previously observed in *Shaker* (Claydon *et al.* 2007) and other Kv channels (Fedida *et al.* 1996; Shieh *et al.* 1997; Wang *et al.* 1999; Wang & Fedida, 2001; Lee *et al.* 2003). The time to peak $I_{g,on}$ was very brief, ∼0.3 ms at +10 mV, and it decreased to ∼0.2 ms at +80 mV (Fig. 5*D*). The decay of $I_{g,on}$ was also fast, ∼2 ms at 0 mV and ∼0.3 ms at +80 mV (Fig. 4*B*).

The most striking difference between Kv3.2b and other channels is that only one charge system is required to account for the time course of $I_{g,on}$ (Figs 2–4) and the voltage dependence of Q_{on} (Fig. 3*C*). The existence of two gating charge systems in *Shaker* channels is necessitated by the presence of a slowly decaying component of $I_{g,on}$ at intermediate depolarizations and the double Boltzmann distribution of the Q_{on}–V relationship (Bezanilla *et al.* 1994). In Kv1.5 channels, the charge–voltage relationship was also best fitted with a double Boltzmann function, and the decaying phase of $I_{g,on}$ at intermediate depolarizations exhibits clearly biphasic waveforms due to the separation of the voltage-dependent parameters of two charge systems (Hesketh & Fedida, 1999). However, Kv3.2b demonstrated a monophasic single exponential decay of $I_{g,on}$ at all tested potentials (Fig. 4*A*) and a symmetrical Q_{on}–V relationship, well fitted to a single Boltzmann function (Figs 3*C* and 4*C*). Although these data can be described using a single charge system, it is possible that the voltage-dependent parameters are such that two charge systems with sufficiently similar half-activation potentials and forward kinetics overlap each other sufficiently to produce a smooth single Boltzmann charge distribution.

Kv3.2b off-gating currents

The $I_{g,off}$ of Kv3.2b channels remains qualitatively similar to that observed in *Shaker* and other Kv channels (Perozo *et al.* 1992, 1993; Chen *et al.* 1997; Yang *et al.* 1997; Wang *et al.* 1999; Wang & Fedida, 2001), and specifically the slowing of gating charge return at more positive potentials was retained. In these channels a slow gating step associated with channel opening, but carrying little charge, is responsible for slowed off-gating currents on repolarization as this step is traversed in the opposite direction. Consistent with this idea, the Q_{off}–V curve for the return of gating charge on repolarization in Kv3.2b channels is negatively shifted by about −70 mV in respect to the Q–V curve during depolarization (Fig. 3*C*). However, the $V_{1/2}$ of the Kv3.2b Q_{off}–V curve is at −81 mV about 15 mV less negative than that of Kv1.5 channels (Wang & Fedida, 2001), so that when the membrane was repolarized to −100 mV, only about 10% of the charge was not captured during the 12 ms repolarizing pulse, much less than the ∼40% charge 'loss' observed in Kv1.5 channels. Thus, the lack of gating charge slowing seen in Kv3.1 expressed in *Xenopus* oocytes (Shieh *et al.* 1997) and Kv3.2b P468W expressed in HEK cells (Yeung *et al.* 2005) is probably due to the nature of the expression system, combined with the voltage-dependent kinetics of the mutant channels and the potentials used to study them, rather than an inability of the charge to return slowly in Kv3 channels. In the case of Kv3.2b P468W, this non-conducting mutant is analogous to *Shaker* P473W (Hackos *et al.* 2002*b*). As P468 is one of the components of the PVP motif that forms the 'gating hinge' in Kv channels (Hackos *et al.* 2002*a*; Labro *et al.* 2003; Sukhareva *et al.* 2003; Long *et al.* 2005), the mutation from P to W prevents channel opening, which is required to see charge slowing on repolarization. Preliminary gating current data obtained from Kv3.1 channels expressed in HEK cells appear very similar to Kv3.2b gating currents in showing charge slowing (authors' unpublished data), which suggests that slowed off-gating currents upon repolarization are generally observed in Kv channels.

Structural considerations in Kv3 gating

The number of charged residues in the S4 segment is an obvious difference in the structure between Kv3 and *Shaker* and its mammalian homologous channels. A valine residue in Kv3.2b channel replaces the lysine at the cytoplasmic end of S4 (K380) in *Shaker*. However, the effect of mutating lysine to valine at this residue on the *Shaker* gating current has not been tested. Exchange of the cytoplasmic half of S5 between Kv3.1 and Kv2.1 channels significantly affected the kinetics of deactivation and $I_{g,off}$, suggesting that S5 participates in the conformational rearrangements associated with the concerted step(s) in channel activation and early step(s) in deactivation (Shieh *et al.* 1997), but no effect on $I_{g,on}$ was observed. Our data from Kv3.2b P468W showed little change in $I_{g,on}$ (Yeung *et al.* 2005) when compared with the data here from wild-type channels, suggesting that charge movement during activation is not influenced significantly by alterations in the gate region of the pore. Interestingly, a recent study of the interaction of S4 with S5 and S6 revealed that a group of mutants located at the interface between the voltage-sensing and pore domains in the Kv1.2 structure perturbed the voltage dependence of activation and induced a pronounced slowing of the relaxation of $I_{g,on}$ in *Shaker* channels (Soler-Llavina *et al.* 2006), suggesting the importance of the interface between the voltage-sensing and pore domains in influencing the kinetics of charge movement during activation.

Mechanism of action of BDS-II

BDS toxins apparently bind to the voltage-sensing domains, S3b and S4, and stabilize them in their resting state, which results in a positive shift of the voltage dependence of activation and slowing of the activation kinetics (Yeung *et al.* 2005). The gating current results from Kv3.2b further support this mechanism by showing that the voltage dependence of the charge movement was shifted by about +23 mV in the presence of 1 μM BDS-II (Fig. 6), without a change in the slope of the relationship. The unchanged slope factor (k) indicated that the effective valency of gating was not altered by BDS-II. Also, a single Boltzmann function was still adequate to fit the Q–V relationship in the presence of BDS-II (Fig. 6), implying that this concentration of BDS-II was sufficient to affect all the apparent charge movement. This result also suggests that BDS-II inhibited the displacement of gating charges in an independent fashion, as suggested for hanatoxin (Lee *et al.* 2003; Swartz, 2007).

One reason for the use of BDS-II in the present experiments was the possibility that it might affect multiple charge systems in Kv3.2 channels differentially, and convert the single Boltzmann charge distribution seen in control to a distribution best fit with a double, or even triple Boltzmann function. This proved not to be the case and supports the idea that a single charge system can explain Kv3.2 gating under the conditions of our experiments and may contribute to the very rapid activation of channels seen physiologically.

Despite this, there were complex changes observed in the kinetics of $I_{g,on}$, with an initial fast phase of on-gating current and the appearance of a second, slower phase. As the voltage dependence of the time constant for the fast decaying component of $I_{g,on}$ was also shifted by BDS-II (Fig. 5*C*), it is hard to explain the fast decaying component as the movement of unbound subunits. The slow phase that appeared in the on-gating currents was more pronounced over the potential range between +20 and +80 mV, and this feature may account for the voltage-dependent slowing of ionic current activation (Yeung *et al.* 2005). Interestingly, BDS-II affected $I_{g,on}$ elicited by relatively weak depolarizations ($\leq +10$ mV), although $I_{g,on}$ transients were small, and at these potentials, the ratio of Q_{off} over Q_{on} was almost equal to 1 (Fig. 5*E*). In the presence of BDS-II the Q_{off} became significantly larger than Q_{on} over a broad range of voltages (Fig. 5*E*), with a maximum ratio of ~3. This ratio diminished again at the most positive potentials studied (+100 mV). The ultimate fate of the $I_{g,on}$ in the presence of BDS-II at intermediate potentials is unclear. The fact that the charge return was complete upon repolarization (Fig. 6) suggests that there was a slowed movement of voltage sensor domains in response to depolarization that was not differentiated from the baseline currents. This is reminiscent of the inability to record immobilized gating charge upon repolarization in Kv1 channels (Fedida *et al.* 1996; Olcese *et al.* 1997) which nevertheless becomes re-available for the next depolarization.

In contrast to the effect on $I_{g,on}$, the $I_{g,off}$ was unaffected by BDS-II. Both the voltage dependence of charge return and the time constant for the relaxation of $I_{g,off}$ remained almost unchanged from the control (Fig. 6), except for a positive potential shift coupled with $I_{g,on}$. This is in good agreement with ionic tail current data from Kv3.1 with BDS-I and BDS-II which shows little effect on the rate of deactivation. But it is different from the reported action of hanatoxin on Kv2.1 ionic current deactivation, which suggests a re-association to channels as they deactivate (Swartz & MacKinnon, 1997*a*,*b*; Lee *et al.* 2003). Two possible explanations for BDS toxins are that they might remain bound to the channel protein during closing, but cannot influence the deactivation process due to the independence of their binding site(s) from the structural elements that regulate deactivation. Alternatively, the toxins may dissociate from the channel after activation, at some time before closing. It seems unlikely that the toxin is actually expelled during closing, since, for most agents like drugs that block open ion channels, the expulsion of

an exogenous agent usually slows the process of closing somewhat. These hypotheses remain to be tested by further experimentation.

References

Bezanilla F, Perozo E, Papazian DM & Stefani E (1991). Molecular basis of gating charge immobilization in *Shaker* potassium channels. *Science* **254**, 679–683.

Bezanilla F, Perozo E & Stefani E (1994). Gating of *Shaker* K^+ channels. II. The components of gating currents and a model of channel activation. *Biophys J* **66**, 1011–1021.

Bezanilla F & Stefani E (1994). Voltage-dependent gating of ionic channels. *Annu Rev Biophys Biomol Struct* **23**, 819–846.

Brew HM & Forsythe ID (1995). Two voltage-dependent K^+ conductances with complementary functions in postsynaptic integration at a central auditory synapse. *J Neurosci* **15**, 8011–8022.

Chen FSP, Steele D & Fedida D (1997). Allosteric effects of permeating cations on gating currents during PK^+ channel deactivation. *J Gen Physiol* **110**, 87–100.

Claydon TW, Vaid M, Rezazadeh S, Kwan DC, Kehl SJ & Fedida D (2007). A direct demonstration of closed-state inactivation of K^+ channels at low pH. *J Gen Physiol* **129**, 437–455.

Diochot S, Schweitz H, Beress L & Lazdunski M (1998). Sea anemone peptides with a specific blocking activity against the fast inactivating potassium channel Kv3.4. *J Biol Chem* **273**, 6744–6749.

Fedida D, Bouchard R & Chen FSP (1996). Slow gating charge immobilization in the human potassium channel Kv1.5 and its prevention by 4-aminopyridine. *J Physiol* **494**, 377–387.

Hackos DH, Chang TH & Swartz KJ (2002*a*). Scanning the intracellular S6 activation gate in the *Shaker* K^+ channel. *J Gen Physiol* **119**, 521–532.

Hackos DH, Chang TH & Swartz KJ (2002*b*). Scanning the intracellular S6 activation gate in the *Shaker* K^+ channel. *J Gen Physiol* **119**, 521–532.

Hesketh JC & Fedida D (1999). Sequential gating in the human heart K^+ channel, Kv1.5, incorporates Q1 and Q2 charge components. *Am J Physiol Heart Circ Physiol* **277**, H1956–H1966.

Labro AJ, Raes AL, Bellens I, Ottschytsch N & Snyders DJ (2003). Gating of *Shaker*-type channels requires the flexibility of S6 caused by prolines. *J Biol Chem* **278**, 50724–50731.

Lee HC, Wang JM & Swartz KJ (2003). Interaction between extracellular Hanatoxin and the resting conformation of the voltage-sensor paddle in Kv channels. *Neuron* **40**, 527–536.

Lien CC & Jonas P (2003). Kv3 potassium conductance is necessary and kinetically optimized for high-frequency action potential generation in hippocampal interneurons. *J Neurosci* **23**, 2058–2068.

Long SB, Campbell EB & MacKinnon R (2005). Crystal structure of a mammalian voltage-dependent *Shaker* family K^+ channel. *Science* **309**, 897–903.

Luneau C, Wiedmann R, Smith JS & Williams JB (1991). *Shaw*-like rat brain potassium channel cDNA's with divergent 3′ ends. *FEBS Lett* **288**, 163–167.

Martina M, Schultz JH, Ehmke H, Monyer H & Jonas P (1998). Functional and molecular differences between voltage-gated K^+ channels of fast-spiking interneurons and pyramidal neurons of rat hippocampus. *J Neurosci* **18**, 8111–8125.

Miller C (1995). The charybdotoxin family of K^+ channel-blocking peptides. *Neuron* **15**, 5–10.

Olcese R, Latorre R, Toro L, Bezanilla F & Stefani E (1997). Correlation between charge movement and ionic current during slow inactivation in *Shaker* K^+ channels. *J Gen Physiol* **110**, 579–589.

Perney TM & Kaczmarek LK (1997). Localization of a high threshold potassium channel in the rat cochlear nucleus. *J Comp Neurol* **386**, 178–202.

Perozo E, MacKinnon R, Bezanilla F & Stefani E (1993). Gating currents from a non-conducting mutant reveal open–closed conformation in *Shaker* K^+ channels. *Neuron* **11**, 353–358.

Perozo E, Papazian DM, Stefani E & Bezanilla F (1992). Gating currents in *Shaker* K^+ channels. Implications for activation and inactivation models. *Biophys J* **62**, 160–168.

Rudy B, Chow A, Lau D, Amarillo Y, Ozaita A, Saganich M, Moreno H, Nadal MS, Hernandez-Pineda R, Hernandez-Cruz A, Erisir A, Leonard C & De Miera EVS (1999). Contributions of Kv3 channels to neuronal excitability. *Ann N Y Acad Sci* **868**, 304–343.

Rudy B & McBain CJ (2001). Kv3 channels: voltage-gated K^+ channels designed for high-frequency repetitive firing. *Trends Neurosci* **24**, 517–526.

Shieh CC, Klemic KG & Kirsch GE (1997). Role of transmembrane segment S5 on gating of voltage-dependent K^+ channels. *J Gen Physiol* **109**, 767–778.

Soler-Llavina GJ, Chang TH & Swartz KJ (2006). Functional interactions at the interface between voltage-sensing and pore domains in the *Shaker* K_v channel. *Neuron* **52**, 623–634.

Southan AP & Robertson B (2000). Electrophysiological characterization of voltage-gated K^+ currents in cerebellar basket and Purkinje cells: Kv1 and Kv3 channel subfamilies are present in basket cell nerve terminals. *J Neurosci* **20**, 114–122.

Sukhareva M, Hackos DH & Swartz KJ (2003). Constitutive activation of the *Shaker* Kv channel. *J Gen Physiol* **122**, 541–556.

Swartz KJ (2007). Tarantula toxins interacting with voltage sensors in potassium channels. *Toxicon* **49**, 213–230.

Swartz KJ & MacKinnon R (1995). An inhibitor of the Kv2.1 potassium channel isolated from the venom of a Chilean tarantula. *Neuron* **15**, 941–949.

Swartz KJ & MacKinnon R (1997*a*). Hanatoxin modifies the gating of a voltage-dependent K^+ channel through multiple binding sites. *Neuron* **18**, 665–673.

Swartz KJ & MacKinnon R (1997*b*). Mapping the receptor site for hanatoxin, a gating modifier of voltage-dependent K^+ channels. *Neuron* **18**, 675–682.

Taglialatela M & Stefani E (1993). Gating currents of the cloned delayed-rectifier K^+ channel DRK1. *Proc Natl Acad Sci U S A* **90**, 4758–4762.

Wang Z & Fedida D (2001). Gating charge immobilization caused by the transition between inactivated states in the Kv1.5 channel. *Biophys J* **81**, 2614–2627.

Wang Z & Fedida D (2002). Uncoupling of gating charge movement and closure of the ion pore during recovery from inactivation in the Kv1.5 channel. *J Gen Physiol* **120**, 249–260.

Wang LY, Gan L, Forsythe ID & Kaczmarek LK (1998). Contribution of the Kv3.1 potassium channel to high-frequency firing in mouse auditory neurones. *J Physiol* **509**, 183–194.

Wang Z, Zhang X & Fedida D (1999). Gating current studies reveal both intra- and extracellular cation modulation of K^+ channel deactivation. *J Physiol* **515**, 331–339.

Yang Y, Yan Y & Sigworth FJ (1997). How does the W434F mutation block current in *Shaker* potassium channels? *J Gen Physiol* **109**, 779–789.

Yeung SY, Thompson D, Wang Z, Fedida D & Robertson B (2005). Modulation of Kv3 subfamily potassium currents by the sea anemone toxin BDS: significance for CNS and biophysical studies. *J Neurosci* **25**, 8735–8745.

Acknowledgements

This work was supported by operating grants to D.F. from the Canadian Institutes of Health Research (CIHR) and the Heart and Stroke Foundation of BC and Yukon, and to B.R. from the MRC and The Wellcome Trust. We are very grateful to Dr David Steele for expert technical assistance in preparing channel constructs and Fifi Chiu and Kyung Hee Park for help with cell culture.